

Evidence for Long-Lasting Electrical Leader Discharges in Non-Specular Meteor Trails Observed In the Summer Polar Upper Mesosphere

Young-Sook Lee^{1,2}, Sheila Kirkwood³, Young-Sil Kwak^{1,4} and Jaejin Lee^{1,4}

¹Korea Astronomy and Space Science Institute, 776 Daedeokdae-ro, Daejeon, Korea

²Earth and Space Science and Engineering, Lassonde School of Engineering, York University, Toronto, Canada

³Swedish Institute of Space Physics, Box 812, SE-981 28, Kiruna, Sweden

⁴Department of Astronomy and Space Science, University of Science and Technology, Daejeon, South Korea

ABSTRACT: Unusual, non-specular, fast-moving meteor trail echoes are observed in the summer polar upper mesosphere near 90 km. Usually, at mid-latitudes, field-aligned irregularities cause non-specular trails, while in the polar region long-lasting irregularities are possibly sustained by charged meteor dust. The unusual meteor trails propagate downward and upward at speeds of 3.3-6.4 km s⁻¹ along a slanted path length of 10.4 km between 87-93 km altitudes, merging in the middle and lasting for 8-10s. Here we propose that an electrical discharge is responsible for these trails. The corresponding horizontal electric field for the observed speeds is estimated up to 16.3 V m⁻¹ at 90 km. Both the long-lasting merging of two fast-moving plasma trails and the modest speed compared to those (~10⁴-10⁵ m s⁻¹) of lightning leader process and of jets (< 400 ms) occurring above thunderclouds likely suggest a new type of meteor-trail leader discharge occurring in the summer polar upper mesosphere.

I. Introduction

In the summer polar mesosphere, there are meteor-related phenomena occurring in the following altitudinal hierarchy: polar summer meteors occurring at 90±10 km [Younger *et al.*, 2009]; polar mesospheric summer echoes (PMSE) occurring at 80-90 km and lasting for minutes to 1-2 hours [Cho and Rottger, 1997]; noctilucent clouds (NLCs or polar mesospheric clouds, PMC) which peaked at 82 km and range from 75-85 km [Cho and Rottger, 1997]. A meteor is a luminous phenomenon occurring through the passage of a meteoroid which penetrates into the Earth's upper atmosphere at 90-120 km at a speed up to 70 km s⁻¹. At the ablation of a meteoroid, meteoric dust or smoke particles are deposited mainly in the upper mesosphere. From meteors, radars can observe head echoes in front of the meteoroid, specular echoes due to meteor trajectories perpendicular to the radar beam, and non-specular echoes from meteor trails [Chau *et al.*, 2014].

Several experimental studies have reported significant levels of electric field fluctuation or strong vertical electric field (0.1-3 V m⁻¹) observed in NLC and PMSE layers [Holzworth and Goldberg, 2004; Shimogawa and Holzworth, 2009]. Horizontal supersonic neutral bursts (500-1500 m s⁻¹) accompanied with an enhanced O(¹S) emission rate (100-170 kR, horizontally integrated) at a wavelength of 557.7 nm were observed by the Wind Imaging Interferometer on UARS satellite. The supersonic bursts were suggested as possibly occurring in strong electric field (> 14-173 V m⁻¹) at 73-85 km, coexisting with PMC and PMSE [e.g., Lee and Shepherd, 2010; Lee *et al.*, 2014]. The meteors or meteoric dust are known for playing a crucial role in producing upper-atmospheric electrical discharges, so called sprites and jets, which are caused by electro-static fields created by and above thunderstorms [Zabotin and Wright, 2001; Pasko *et al.*, 1998]. However, so far radar observations have not been reported of the upper atmospheric electrical discharge, probably since the well-known forms (e.g. sprites or jets) last less than a few hundreds of milliseconds so that only the high-resolution optical instruments might be able to observe.

At mid-latitudes, meteor trails can lie close to parallel with the geomagnetic field and field-aligned plasma irregularities have been found to explain their behaviour. For high latitudes, the presence of charged meteor dust has been proposed to maintain long-duration irregularities by decreasing the diffusion coefficient (m²s⁻¹) [e.g., Kelley, 2004; Chau *et al.*, 2014]. Thus, so far many studies have likely focused on identifying the mechanism to detain meteor trails to be barely diffusive. Instead, we observe fast-moving, non-specular meteor trails regardless their orientation aligned against the geomagnetic field. This study for the first time reports a discovery of the evidence of electrical leader discharge in the meteor trails with a modest (compared to sprites or meteoroids) speed (~ 3-7·10³ m s⁻¹), moving simultaneously both horizontally downward and upward. It is interesting to estimate how far and fast the meteor trails move across the spatial domain, and to understand what force continuously exerts on the meteor trail to move at such speeds.

II. Data Analysis And Results

2.1 Experiments

Esrance MST radar (ESRAD) operates at a frequency of 52 MHz, i.e. a wavelength of 5.77 m, and is installed in Kiruna (67.8°N, 20.04°E), Sweden. The ESRAD radar is set up as six-spaced receivers, with antenna subarrays in two rows aligned in the W-E direction and three columns aligned in the N-S direction, so that receivers are arranged in west-to-east with a first row of 1, 2, 3 (north) and a second row of 6, 5, 4 (south). For more details, of the radar and operating modes, see *Kirkwood et al.* [2007]. Here we use the fca_150 mode, which has height aliasing at every 32 km. The height aliasing can be resolved by considering that the meteor occurrence peak is usually observed at 90 ± 10 km [Younger et al., 2009], and statistically the frequency of occurrence on the meteor-originated radar echoes below 80 km is about 1 in 10,000 [Park and McIntosh, 1967].

2.2 Peculiar motion of non-specular meteor trail in a direction

So far, many studies have reported about non-specular meteor trails, which are relatively static in aspects of vertical and horizontal motions of plasma clouds, but only subject to a diffusion at either middle or high latitude [Oppenheim et al., 2003; Dyrud et al., 2007; Chau et al., 2014]. At ESRAD, we observe instead long-lasting fast-moving meteor trail echoes downward and upward to the opposite directions. ESRAD has interferometric capability to resolve the spatial location echoes (within zenith angles of about 10°) and the speed of growth of meteor trails. Figure 1a shows the signal power of unusual non-specular meteor trail echoes from receiver no. 5. The signal power is greater than that of normal PMSE at 30-35 dB above the noise level (not shown here). Meteor trail echoes start initially by descending from the top (93 km) and later by ascending, launched from below (87 km), observed at 18:54:35 UT on Jun 22, 2006 (day = 173). There is no head echo apparent [Dyrud et al., 2002]. The relative time is a time distance from the measurement start, within the record length of 28 s. Three time intervals are defined: first for only downward propagation, observed from a relative time of 16.7-18.7s, second, for upward propagation launched at an interval of 18.1-18.7 s and third, for merging of the two propagating trails at an interval of 18.1-24.5 s.

The signal received by the radar receiver is composed of complex numbers, giving amplitude and phase information. The angle (or phase) difference ($\delta\phi$) of coherent signals acquired by two receivers gives information on the zenith angle of the path to the scatterer (signal source), in the direction between the receivers, providing a fundamental interferometric key to resolve the spatial extension of the meteor trail echoes [Skolnik, 1962, p. 222-223]. Figure 1b shows phase differences from the reference receiver 5 (Rx5). Phase difference between receivers 5 and 4 (Rx5-4) and 5 and 6 (Rx5-6) are close to zero (or 2π) and have the almost same value through all altitudes. This indicates the position of the scatterers is approximately symmetric with respect to the N-S zenith plane and constant with height in the east-to-west direction. The phase difference (Rx5-2) between Rx5 and Rx2 shows a larger phase difference in the upper part changing steadily to a smaller phase difference in the lower part, corresponding to a slanted trail path in terms of altitude. Thus, the plasma clouds causing the echoes are likely elongated between north and south along a slope so that the top is biased to the north, and the bottom to the south. Therefore, the plasma clouds initially (at 16.7 s in relative time) likely propagate from the top (93 km) and the north, extending horizontally downward and southward. While, after 1.4 s (at 18.1 s) from the bottom the plasma clouds propagate horizontally upward and northward along the slanting path. Finally, propagating trails from opposite directions merge at the middle height of ~89 km.

2.3 Estimates of spatial extension and the dynamics

The spatial extension and propagating speed of the meteor trail can be estimated using the phase difference (interferometric) capability of the radar. The phase difference of a signal received in the two receivers (e.g. Rx5-Rx2, south-to-north arrangement, $d = 32$ m) can provide an angle θ to the target by a formula $\sin\theta = \frac{\delta\phi}{2\pi d/\lambda}$, where $\lambda =$ wavelength (5.77 m) [Skolnik, 1962, p. 222-223]. The spatial extension and propagating speed of the meteor trail can be estimated using the phase difference (interferometric) capability of the radar. Figure 2a shows the geometry of the angle of arrival using two receivers (e.g., Rx5 and Rx2, south-to-north arrangement, $d = 32$ m) [Skolnik, 1962, p. 222-223]. If the signal arrives from a direction θ with respect to the normal to the baseline, the angle θ has a relationship as below with phase difference ($\delta\phi$) in a signal received in the two receivers,

$$\sin\theta = \frac{\delta\phi}{2\pi d/\lambda}, \quad (1)$$

where $\lambda =$ wavelength (5.77 m). Thus the phase difference of a signal received in the two receivers (e.g. Rx5-Rx2) can provide an angle θ to the target. Figure 2b shows the geometry of the trail path for the dynamical meteor trail echoes as shown in Figure 1a. From equation 1, phase differences of in average $\delta\phi_1 = 2.2 \pm 0.4$, $\delta\phi_2 = 3.4 \pm 0.3$ and $\delta\phi_3 = 5.2 \pm 0.2$ radians (top-left panel of Figure 1b) give arrival angles of signal in

$\theta_1 = 0.063$, $\theta_2 = 0.097$, $\theta_3 = 0.149$ radians at 87 km, 89 km and 93 km, respectively. Spatial distances derived using $r \sin \theta$ result in $l_1 = 5.48$ km, $l_2 = 8.7$ km and $l_3 = 13.93$ km for horizontal displacements from ESRAD at 87 km, 89 km and 93 km, respectively. The inclination of the geomagnetic field near the Kiruna becomes an angle of 78° [http://geokov.com/education/magnetic-declination-inclination.aspx]. The lower and upper trail paths having inclination angles of $\alpha_1 \approx \alpha_2 \approx 30^\circ$ form angles of $\beta_1 \approx \beta_2 \approx 70^\circ$ to the geomagnetic field, respectively. From the far left slopes of the echoes as shown in Figure 1a it apparently takes 2 s for propagating downward from 93-89 km altitudes, a distance of $p_2 = 6.56$ km and takes 0.6 s for propagating upward from 87-89 km, a distance of $p_1 = 3.85$ km, and then the downward and upward propagating trails merge at 89-90 km. The merge of downward and upward propagating plasmas persists for a duration of 5.7 s. The downward and upward propagations along trail paths are initiated at speeds of 3.3 km s^{-1} and 6.4 km s^{-1} , gradually decreasing down to 841 m s^{-1} and 602 m s^{-1} at the end, respectively. The propagating speed is estimated assuming the trails propagating in straight paths, so that if the trail paths are somewhat bent, which is more realistic and unable to be estimated, actual speeds should be larger than the estimated.

III. Phenomena In Nature With The Comparable Speed

Non-specular echoes are usually explained with two mechanisms: one is related to field-aligned irregularities mainly occurring in mid-latitude [e.g., *Oppenheim et al.*, 2003; *Dyrud et al.*, 2007]; the second one is irregularities in the presence of charged meteor dust usually occurring in the polar region, lasting for up to a few tens of seconds [e.g., *Kelley*, 2004; *Chau et al.*, 2014]. However, up to now, in radar observations, there have not been reported about fast moving meteor trails at such a high speed ($3.3\text{-}6.4 \text{ km s}^{-1}$) as observed in this study in the upper mesosphere (80-100 km) in any latitude region. In the meanwhile, there seem to be many optical observations of similar speeds, although lasting for shorter duration. *Suszczynsky et al.* [1999] observed a bright meteor, followed by sprite and then by jets moving in the opposite direction from 80-84 km at a speed of $70\text{-}130 \text{ km s}^{-1}$. The velocity is too slow to suggest the luminous phenomenon produced by a pure electrical current flow in a fully ionized channel. However, the luminous jet moving backward along the trajectory of the meteor would be associated with the presence of meteor ionization trail, likely involving a complicated generation mechanism [*Symbalisy et al.*, 2000]. For this, *Spurný and Cepelcha* [2008] suggested that strong electric field might be developed in a meteor trail by charge separation between the inside and surface of meteoroid during its flight. This idea also can elucidate why non-fragile meteoroid go through abnormal explosive fragmentation in too-low atmospheric pressure. As shown in Figures 1-2, the fast moving plasma clouds we observe move with such fast speeds that they cannot be explained with either ambipolar diffusion process (e.g. diffusion coefficient of $1 \text{ m}^2 \text{ s}^{-1}$ near 90 km) [*Chau et al.*, 2014] or aerodynamics. Therefore, an energy source needs to be sought for, which firstly is capable of putting the plasma clouds in motion both upward and downward at such a fast speed, and secondly leads to the plasma dynamics persisting for over 8 s.

IV. Meteor Trails As An Electrical Discharge Phenomenon

With ESRAD coherent radar having a 3 m Bragg scale wavelength [*Briggs*, 1984], it is not possible to see the motion of single ions or electrons. In addition, the radial speed of the scatterers cannot be unambiguously measured from the Doppler shift due to the folding effect by the Nyquist frequency. So the meteor trail propagation speed is the best indicator of a plasma cloud speed or mean ion speed. The plasma speed along the slanting path can be proportional to an electric field if that is assumed as the energy source. The horizontal electric field (\vec{E}) component of the slanted trail path can be estimated using a formula $\vec{E} = \frac{m_i v_{in} \vec{v}}{q}$, where q is the electric charge of the electron, \vec{v} is ion or neutral velocity (m s^{-1}), m_i is the mean ion mass obtained from MSIS-90 [*Hedin*, 1987], and v_{in} is the ion-neutral collision frequency [*Lee and Shepherd*, 2010]. As shown in Figure 2, upper and lower trail paths with an inclination angles of $\sim 30^\circ$ gives horizontal components of 2.84 km s^{-1} and 5.5 km s^{-1} derived from velocities of 3.64 km s^{-1} and 7.6 km s^{-1} , respectively. Horizontal components of electric field correspond to values of 8.3 V m^{-1} and 16.3 V m^{-1} at 90 km. The electric fields highly exceed the conventional breakdown field, for example, about $8\text{-}10 \text{ V m}^{-1}$ at 90 km [*Pasko et al.*, 2013]. The high angle ($\sim 70^\circ$) of propagating trail path to the magnetic field likely implies that the plasma trail cannot be magnetized in the strong electric field but pass through the magnetic field.

Therefore, such high speeds of meteor trail echoes are comparable with those of leader process of tropospheric lightning and jet events occurring above thunderclouds. Lightning discharge is explained with two principal modes of the streamer and the leader. The leader takes in charge at a high gas temperature, high ionization and high electric conductivity, propagating at velocities of $10^5\text{-}10^6 \text{ m s}^{-1}$. The streamer, on the other hand, has cold gas temperature, low ionization, and low electric conductivity, propagating at velocities of 10^7 m s^{-1} [*Neubert et al.*, 2011]. In lightning, many streamers explore the path for the leader, preceding leader process [*Raizer*, 1997, p. 364]. *Pasko et al.* [2002] reported blue jets launched upward from thunder cloud tops at

speeds which varied from 50 km s^{-1} to 270 km s^{-1} . *Su et al.* [2003] observed a gigantic jet at an upward speed of 26 km s^{-1} and 120 km s^{-1} and subsequently decreasing to 13 km s^{-1} above thunderclouds terminated at 60 km and 68 km. The speed of jets is consistent with known speeds of the leader process in conventional lightning [*Uman*, 2001; *Pasko et al.*, 2002].

Meteor trail echoes as shown in Figure 1a are possibly attributed to leader discharges based on two distinct features: one is the speed level ($3.3\text{-}6.4 \text{ km s}^{-1}$) and the estimated electric fields, and another is the merging of two trails at the middle point after propagating in opposite directions. According to *Spurný and Cepelcha* [2008], a meteoroid develops charge separation during its penetration, positively charged on the surface and negatively inside, and at last leads to electrical charge separation in the meteor trail. As a result, the plasma cloud at the top will be negatively charged and the one at the bottom, if it is the final vaporization of the meteor, will be positively charged. Figure 3 shows a schematic diagram of leader discharges according to time intervals of the non-specular echoes as shown in Figure 1, corresponding to, firstly, downward propagation only occurring (16.7s – 18.7s), secondly upward propagation launched (18.1s-18.7s), and finally persistent merging of downward and upward plasma (18.1s – 24.5s), respectively. The persistent merging of downward and upward running trails provides an outstanding signature of the meteor trail propagating in a hot plasma gas of a highly conductive channel. By theory, the property of cold plasma is transient in lasting for μs to ms from experimental results [*Becker et al.*, 2004], while the hot plasma is usually capable of increasing neutral and ion temperature up to electron temperature. According to *Becker et al.* [2004], for example, a lightning stroke can increase temperature up to $30,000^\circ\text{C}$ [*Uman*, 2001]. Therefore, the meteor trail discharge can play a role of heating the mesospheric air. However, to see the temperature modulation effect is beyond the scope of the current paper.

As classifying breakdown mechanisms in terms of pd values (p is pressure in Torr, d is electrode distance in cm), streamer breakdown can be achieved based on $4000 < pd < 10^5 \text{ Torr} \cdot \text{cm}$ and leader breakdown needs to be over $10^5 \text{ Torr} \cdot \text{cm}$ [*Pasko et al.*, 2013]. For streamer and leader breakdowns to occur at $\sim 90 \text{ km}$ requires gaps of 20 - 512 km and $> 512 \text{ km}$, respectively, due to the low pressure of 0.002 Torr at the altitude ($760 \text{ Torr} = 760 \text{ mmHg} = 1 \text{ Atm} = 1.013 \text{ bar}$). The observed leader discharges with a vertical gap $< 10 \text{ km}$ might be difficult to generate in terms of the mesospheric pressure. There is a similar difficulty in explaining the initiation of traditional sprites caused by the relativistic runaway breakdown, which should need a long avalanche distance l_a at low pressures (i.e., at $70 \text{ km } l_a = 370 \text{ km}$) [*Gurevich and Zybin*, 2001]. As in lightning process, streamer discharge normally precedes leader phenomenon. Thus, streamer-to-leader transition process requires a persistent supply of electric field [*Pasko*, 2003]. In this aspect, the long-lasting trail leader discharge suggested here would represent an unprecedented observation since, near 90 km, only very transient electric field (\sim a few 10s of milliseconds) is required for sprites and even the traditional jet as a leader phenomenon usually observed in the stratosphere extending up to 60 km lasts very short duration ($< 400 \text{ ms}$) [*Pasko et al.*, 2002; *Su et al.*, 2003]. This study suggests, for the observed non-specular meteor trail, discharge as a new type of meteor trail leader. Therefore, it is a challenge to understand how the strong electric field can be supplied for a relatively long duration of about 10 s, including the unobserved altitude region over 93 km. This is much longer lasting than the leader process of traditional jet occurring above thunderstorms (100-400 ms) [*Pasko et al.*, 2002; *Su et al.*, 2003].

V. Conclusions

Unusual dynamical non-specular meteor trails moving at a leader discharge speed are observed by ESRAD at Kiruna, Sweden. Interferometric capability of the radar allows us to resolve the spatial geometry of the meteor trail as horizontally and vertically elongated between 87-93 km, and the speed of the propagating plasma trails.

1. The vertical profile of the non-specular trail is extended along a slope having horizontal displacements as long as 10.4 km from 87-93 km, not field-aligned but at a high inclination angle ($64^\circ\text{-}71^\circ$) to the geomagnetic field.
2. Downward and upward propagating speeds are estimated as 3.3 km s^{-1} and 6.4 km s^{-1} , decreasing to 841 m s^{-1} and 602 m s^{-1} , respectively, assumed the propagating path is straight. The trail speed can be achieved by plasma acceleration in a strong electric field. The speeds correspond to horizontal electric fields up to 16.3 V m^{-1} at 90 km, which exceeds conventional breakdown field.
3. The downward and upward propagating plasmas come to merge in the middle of the path, which is evidence that the electrical discharge is a leader discharge forming a hot plasma channel.
4. It is remarkable that long-lasting electric field can be sustained for 8-10 s, in contrast to any electrical leader discharge occurring above thunderstorms ($< 400 \text{ ms}$). Therefore, this study suggests the non-specular trail discharge is a new type of meteor-trail leader discharge occurring in the summer polar upper mesosphere.

Acknowledgements

This paper is based on research sponsored by the “Solar Behavior and Near Earth Space Exploration” project and the Air Force Research Laboratory (under agreement FA2386-14-1-4004). It also received basic research funding from Korea Astronomy and Space Science Institute (KASI). ESRAD is a joint venture between Swedish Institute of Space Physics and Swedish Space Corporation, Esrange. The contact information for ESRAD data is provided at <http://www.irf.se/program/paf/mst/>.

References

- [1]. Becker, K.H., U. Kogelschatz, K.H. Schoenbach, R.J. Barker (2004), *Non-Equilibrium Air Plasmas at Atmospheric Pressures*, Institute of Physics Publishing: London (2005), Distributor: Francis & Taylor, CRC Press.
- [2]. Briggs, B. H. (1984), The analysis of spaced sensor records by correlation techniques, in: *Handbook for MAP, vol. 13, SCOSTEP Secr.*, Univ. of Ill., Urbana, 166–186.
- [3]. Chau, J. L., I. Strelnikova, C. Schult, M. M. Oppenheim, M. C. Kelley, G. Stober, and W. Singer (2014), Nonspecular meteor trails from non-field-aligned irregularities: Can they be explained by presence of charged meteor dust?, *Geophys. Res. Lett.*, 41, doi:10.1002/2014GL059922.
- [4]. Cho J.Y.N and JürgenRöttger (1997), An updated review of polar mesosphere summer echoes' Observation, theory, and their relationship to noctilucent clouds and subvisible aerosols, *J. Geophys. Res.*, 102, No.D2, 2001-2020.
- [5]. Dyrud, L. P., M. M. Oppenheim, S. Close, and S. Hunt (2002), Interpretation of non-specular radar meteor trails, *Geophys. Res. Lett.*, 29(21), 2012, doi:10.1029/2002GL015953.
- [6]. Dyrud, L. P., E. Kudeki, and M. Oppenheim (2007), Modeling long duration meteor trails, *J. Geophys. Res.*, 112, A12307, doi:10.1029/2007JA012692.
- [7]. Hedin, A. E. (1987), MSIS-86 thermospheric model, *J. Geophys. Res.*, 92, 4649–4662, doi:10.1029/JA092iA05p04649.
- [8]. Holzworth, R. H., and R. A. Goldberg (2004), Electric field measurements in noctilucent clouds, *J. Geophys. Res.*, 109, D16203, doi:10.1029/2003JD004468.
- [9]. Kelley, M. C. (2004), A new explanation for long-duration meteor radar echoes: Persistent charged dust trains, *Radio Sci.*, 39, RS2015, doi:10.1029/2003RS002988.
- [10]. Kirkwood, S., I. Wolf, H. Nilsson, P. Dalin, D. Mikhaylova, and E. Belova (2007), Polar mesosphere summer echoes at Wasa, Antarctica (73°S): First observations and comparison with 68°N, *Geophys. Res. Lett.*, 34, L15803, doi:10.1029/2007GL030516.
- [11]. Lee, Y.-S., and G. G. Shepherd (2010), Summer high-latitude mesospheric observations of supersonic bursts and O(¹S) emission rate with the UARS WINDII instrument and the association with sprites, meteors, and lightning, *J. Geophys. Res.*, 115, A00E26, doi:10.1029/2009JA014731.
- [12]. Lee, Y.-S., S. Kirkwood, Y.-S. Kwak, K.-C. Kim and G.G. Shepherd (2014), Polar summer mesospheric extreme horizontal drift speeds during interplanetary corotating interaction regions (CIRs) and high-speed solar wind streams: coupling between the solar wind and the mesosphere, *J. Geophys. Res. Space Physics*, 119, 3883–3894, doi:10.1002/2014JA019790.
- [13]. Neubert, T., O. Chanrion, E. Arnone, F. Zanotti, S. Cummer, J. Li, M. Füllekrug, S. Soula, and O. van der Velde (2011), The properties of a gigantic jet reflected in a simultaneous sprite: Observations interpreted by a model, *J. Geophys. Res.*, 116, A12329, doi:10.1029/2011JA016928.
- [14]. Gurevich A. and K. P. Zybin (2005), Runaway breakdown and the mysteries of lightning, *Physics Today*, May 2005, 37-43.
- [15]. Oppenheim, M. M., L. P. Dyrud, and L. Ray (2003), Plasma instabilities in meteor trails: Linear theory, *J. Geophys. Res.*, 108(A2), 1063, doi:10.1029/2002JA009548.
- [16]. Park, F. R. and B. A. McIntosh (1967), A bright fireball observed photographically by radar and visually, *J. of RASC*, 61 (1), 25-39.
- [17]. Pasko V. P., Inan U. S., and Bell T. F. (1998), Spatial structure of sprites, *Geophys. Res. Lett.*, 25, 2123–2126.
- [18]. Pasko, V. P., M. A. Stanley, J. D. Mathews, U. S. Inan, and, T. G. Wood (2002), Electrical discharge from a thundercloud top to the lower ionosphere, *Nature*, 416, pp. 152-154.
- [19]. Pasko, V. P. (2003), Dynamics of streamer-to-leader transition in transient luminous events between thunderstorm tops and the lower ionosphere. *Eos Trans. AGU - Fall Meet. Suppl.*, 84(46):AE41B–05. Abstract.
- [20]. Pasko, V. P., Jianqi Qin and Sebastien Celestin (2013), Toward Better Understanding of Sprite Streamers: Initiation, Morphology, and Polarity Asymmetry, *Surveys in Geophysics*, 34 (6), 797-830.
- [21]. Raizer, Yu. P. (1991), *Gas Discharge Physics*, Springer-Verlag, Berlin Heidelberg.
- [22]. Shimogawa, M. and R.H. Holzworth (2009), Electric field measurements in a NLC/PMSE region during the MASS/ECOMA campaign, *Ann. Geophys.*, 27, 1423-1430.
- [23]. Skolnik, Merrill (2001), *Introduction to radar systems*, third edition, McGraw-Hill.
- [24]. Spurný, P. and Z. Cepelcha (2008), Is electric charge separation the main process for kinetic energy transformation into the meteor phenomenon?, *A&A* 489, 449–454.
- [25]. Su, H. T., Hsu, R. R., Chen, A. B., Wang, Y. C., Hsiao, W. S., Lai, W. C., Lee, L. C., Sato, M., and Fukunishi, H. (2003). Gigantic jets between a thundercloud and the ionosphere, *Nature*, 423:974–976.
- [26]. Suszcynsky, D. M., R. Strabley, R. Roussel-Dupre, E. M. D. Symbalisty, R. A. Armstrong, W. A. Lyons, and M. Taylor (1999), Video and photometric observations of a sprite in coincidence with a meteor-triggered jet event, *J. Geophys. Res.*, 104(D24), 31,361-31,367.
- [27]. Symbalisty, E.M. D., R. Roussel-Dupre, D. O. ReVelle, D.M. Suszcynsky, V. A. Yukhimuk, and M. J. Taylor (2000), Meteor Trails and Columniform Sprites, *Icarus*, 148, 65.
- [28]. Uman, Martin A. (2001), *The Lightning Discharge*, Dover Publications, New York.
- [29]. Younger, P.T., I. Astin, D. J. Sandford, and N. J. Mitchell (2009), The sporadic radiant and distribution of meteors in the atmosphere as observed by VHF radar at Arctic, Antarctic and equatorial latitudes, *Ann. Geophys.*, 27, 2831-2841.
- [30]. Zabotin, N. A. and Wright, J. W. (2001). Role of meteoric dust in sprite formation, *Geophys. Res. Lett.*, 28(13):doi:10.1029/2000GL012699.

Figures

Figure 1. ESRAD antenna array is composed with 2 rows of 6 antenna segments each with separate receivers: receiver no.1, 2, 3 at 1st row and no. 6,5,4 at 2nd row arranged from west-to-east. The first and second rows are aligned in north-to-south. (a) Non-specular meteor trail echo pattern plotted in power in dB in terms of height (150 m interval) and time (0.027 s interval) only shown for receiver 5 (Rx.5), occurring on June22, 2006

(173) at 18:54:35; (b) Phase difference noted in radian referred to Rx5. Rx.1 was out of order during the data collection. The relative time is a time distance since the measurement started, within the record length of 28 s.

Figure 2. Interferometric interpretation with the arrival angle of the signal received by Rx5 and Rx2 and the phase difference applied for the meteor trail echoes observed at 18:54, June 22, 2006 as shown in Figures 1a-1b. (a) simplified schematic diagram of interferometric radar, adopted from Skolnik [2001, p. 222]. A scatterer (S) is seen from two receivers. The variable of d indicates distance between receivers A and B (e.g., Rx5 and Rx2) to be 32 m for N-S. Length between A and C is $d \sin\theta$, where θ is arrival angle of the signal received from the two receivers. The variable of r is height; (b) In terms of mean phase differences (radian) of $\delta\varphi_{rad1} = 2.2 \pm 0.4$, $\delta\varphi_{rad2} = 3.4 \pm 0.3$, $\delta\varphi_{rad3} = 5.2 \pm 0.2$, signal arrival angles are $\theta_1 = 0.063$, $\theta_2 = 0.097$ and $\theta_3 = 0.149$ in radians and the horizontal trail path lengths are $l_1 = 5.48$ km, $l_2 = 8.7$ km and $l_3 = 13.93$ km, which can be derived by using $l = r \sin \theta$, where r is radius (height). Scatterers' moving path length to be $p_1 \cong 3.85$ km and $p_2 \cong 6.56$ km, the paths inclined by angles of $\alpha_1 = 28.4^\circ$ and $\alpha_2 = 32.8^\circ$. Geomagnetic field inclination of $I = 78^\circ$. Trail paths make angles of $\beta_1 = 73.6^\circ$ and $\beta_2 = 69.2^\circ$ to the magnetic field.

Figure 3. Schematic diagram according to polarity formation and time intervals of the non-specular trails' propagation as shown in Figure 1a: (a) at the top (negative polarity), leader discharge initiated with downward propagating trail; (b) upward discharge launched from below (positive polarity), 1.4s after the downward propagation launched, only regarded for observable trail range with respect to altitudes; (c) the downward/upward propagating trails merge in the middle heights. Speeds V_1 vary from 3.3 km s^{-1} down to 841 m s^{-1} and V_2 are from 6.4 km s^{-1} down to 602 m s^{-1} . Streamers preceding the leader are actually non-visible from ESRAD observation but are depicted by assumption that streamer-to-leader transition occurs in some way [Raizer, 1991].

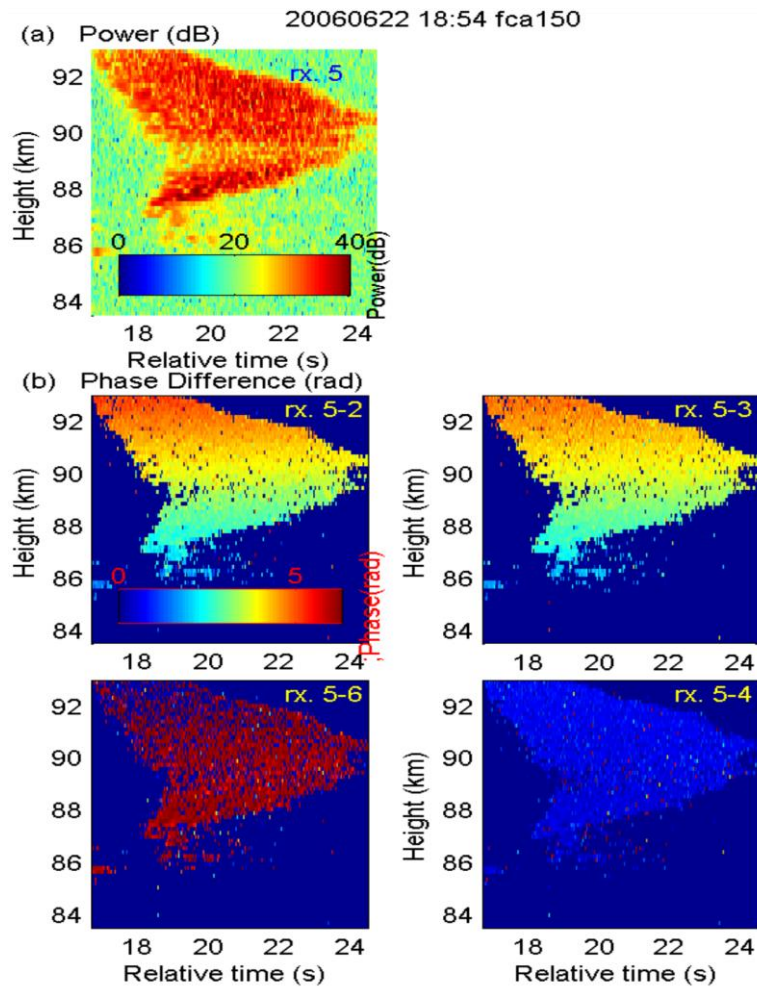


Figure 1.

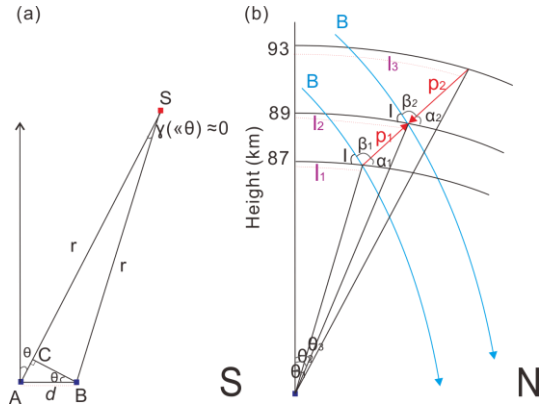


Figure 2.

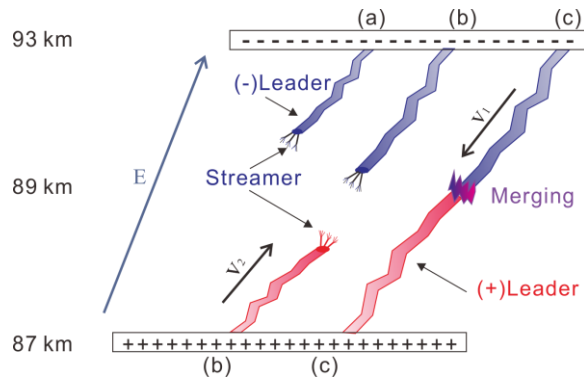


Figure 3.